

Superconducting Cavities and their Applications -

Recent Work at the University of Wuppertal

M. Becks*, A. Brust, H. Chaloupka Δ , M. Hein, S. Haindl, H. Heinrichs, M. Jansen, M. Jeck Δ , N. Klein, U. Klein*, S. Lauterjung, E. Mahner, A. Michalke, N. Minatti, G. Müller, B. Mönter, D. Opie⁺, S. Orbach, M. Peiniger, L. Ponto⁺⁺, H. Piel, A. Pischke Δ , D. Reschke, R.W. Röth, J. Schurr, N. Tellmann, D. Wehler, F. Zander

Fachbereich Physik und Δ Fachbereich Elektrotechnik der Bergischen Universität
D-5600 Wuppertal 1, Gaußstr. 20, West Germany.

*Interatom GmbH., Bensberg, West Germany

⁺Department of Physics, College of William and Mary, Williamsburg, Va. USA

⁺⁺Politechnika Warszawska, Wydz. Chemiczny, Warszawa, Poland

Abstract

This report gives an overview over the work in rf superconductivity at the University of Wuppertal. It references experiments which have been performed and published in the last two years and concentrates on ongoing and as yet unpublished work. Superconducting material studies are described such as Hc₂ measurements on thin Nb₃Sn surface layers and the deposition of such layers on high purity niobium. First results on scanning superfluid thermometry and x-ray mapping on s.c. cavities at high fields are given and the achieved accelerating fields in postpurified single and multicell cavities at 3 GHz are summarized. Out of the field of non-accelerator application of superconducting cavities a high T_C cavity for a compact superconducting hydrogen maser is described and first Q measurements are reported. Finally a new method is introduced to measure the gravitational constant by the use of a superconducting Fabry-Perot cavity and initial experimental results are shown. Not included in this report are major parts of our work such as the improvement program for the cavities of the Darmstadt Recyclotron [1], a superconducting high brightness electron source [2] and the materials processing of high T_C superconductors and the determination of their rf properties [3]. These subjects are treated in the referenced posters and review talks at this workshop.

1. Introduction

Research in rf superconductivity was started in Wuppertal right after the foundation of the new university in 1973. From the beginning our work was guided by applications of superconducting cavities to particle accelerators and to devices for experiments in general physics. The S-band multicell accelerating cavities for the Darmstadt superconducting recyclotron [4] and the K-band TE-mode cavities for the single atom maser [5] are examples of these activities. The discovery of the absence of electron multipacting in cavities of spherical shape [6] and the development of the temperature mapping technique in subcooled helium [7] were important steps on the way to improve the obtainable accelerating fields in niobium cavities. The coating of niobium cavities with Nb₃Sn resulted in the first high T_C accelerating structures [8]. Furnaces for the treatment of niobium cavities at temperatures of up to 1950°C were developed in 1978 [9] and are applied since then to clean cavities of complex shape from chemical residues and to homogenize impurities imbedded in the bulk niobium. Since the pioneering work on the improvement of the thermal conductivity of niobium at Cornell University [10] our furnaces are also used to postpurify niobium cavities designed for high field applications. Studies directed towards the improvement of niobium and Nb₃Sn for the application in high Q and high field cavities have been continued in the two years after the last workshop in Argonne. About one half of the Wuppertal group is presently devoted to investigate rf properties, material processing techniques and applications of the high T_C oxide superconductors. This work is concentrated on YBa₂Cu₃O_{7-δ} and is covered in detail in G. Müller's review [3] and in the poster session [11,12]. Work has been started to develop a high brightness superconducting electron source using a reentrant superconducting 500 MHz niobium cavity with a retractable CsSb cathode on a niobium stem [2]. This subject as well as the postpurification technique applied to the accelerating structures of the Darmstadt recyclotron are also covered in the poster session at this workshop [1] and are therefore not discussed in this summary. The following chapters outline experimental studies on Nb₃Sn layers on high purity niobium, and describe first results on scanning thermometry in superfluid helium and x-ray mapping on single cell cavities at high fields as well as the high field performance of single and multicell postpurified niobium cavities. Two new projects using superconducting cavities in non-accelerator related experiments were started since 1987. The first is an experi-

mental prototyp of a superconducting YBCO cavity for a compact hydrogen maser for space applications oscillating approximately at 1.42 GHz. The basic ideas and the progress of this work is reported. The second of these experiments is a pendulum gravimeter using a superconducting Fabry-Perot cavity. This experiment is designed to investigate a method different from the one used in the classical Cavendish experiment to determine the gravitational constant. First test results are given in the last chapter of this summary.

2. Progress in Nb₃Sn Cavities

In the past years single- and multicell cavities fabricated from reactor grade niobium (RRR = 30) have been coated with Nb₃Sn using the vapor diffusion technique [13]. Compared to niobium cavities improvement factors of about 200 were achieved for the BCS surface resistance (R_s^{BCS}) at 4.2 K. The obtained Q values in the frequency range between 1 and 9 GHz were close to 10^{10} and determined by the residual surface resistance (R_{res}). With the effective surface resistance R_s given by

$$R_s = R_s^{\text{BCS}} + R_{\text{res}} \quad (1)$$

we obtained for R_s^{BCS} and $T \leq 0.7 T_c$ approximately:

$$R_s^{\text{BCS}}(\text{Nb}_3\text{Sn}) = 9.4 \cdot 10^{-5} f^2/T e^{-\alpha T_c/T} \Omega \quad (2)$$

with $\alpha = 2.2$; $T_c = 18$ K the frequency f given in GHz and the temperature T given in Kelvin.

This may be compared to an equivalent parametrization of R_s^{BCS} for niobium:

$$R_s^{\text{BCS}}(\text{Nb}) = 9.0 \cdot 10^{-5} f^2/T e^{-\alpha T_c/T} \Omega \quad (3)$$

with $\alpha = 1.83$ and $T_c = 9.2$ K.

The residual resistance of Nb₃Sn was found to be larger than for niobium and to scale at low surface magnetic fields approximately like

$$R_{\text{res}}(\text{Nb}_3\text{Sn}) = 1.6 \cdot 10^{-8} f^2 \Omega \quad (4)$$

with f given in GHz.

$R_{\text{res}}(\text{Nb}_3\text{Sn})$ increases significantly with increasing surface field. At 3 GHz for example an increase from $1.4 \cdot 10^{-7} \Omega$ to $4.7 \cdot 10^{-7} \Omega$ was observed in going from a very low surface field to 430 Oe. It is interesting to note that the same frequency dependence and an even stronger field dependence of R_s is observed for the high T_c oxide superconductors. Both materials share the feature of a very small coherence length and R_{res} may therefore be dominated by intergrain losses. The residual resistance dependence on the phase purity of the Nb_3Sn layer can vary from one surface preparation to the next if not all parameters have been kept constant. It is of course also influenced by chemical surface impurities from the final cleaning process and by dust particles on the rf surface. Equation (4) can therefore only give a guideline what may be expected after applying the present surface preparation techniques.

The maximum achievable accelerating fields in Nb_3Sn cavities stayed typically below 5 MV/m (surface magnetic field < 225 Oe) and were never observed to be higher than 7.2 MV/m (see Fig. 2). These limiting fields are very similar to those obtained in low purity (RRR = 30) niobium cavities. This is understandable as the observed thermal instabilities result from the same microscopic defects found in niobium cavities. These defects are cooled like in a niobium cavity. A Nb_3Sn cavity is different from a niobium cavity only by its 1 μm thick Nb_3Sn surface layer which is of very low thermal conductivity. This low conductivity may compensate the higher threshold temperature for a thermal instability. We have therefore attempted a better thermal stabilization of normal conducting defects by depositing a very thin ($\leq 1 \mu\text{m}$) layer of Nb_3Sn on a high purity (RRR > 100) niobium cavity [14]. First coating experiments by the standard vapor diffusion process failed in two respects. At first an incomplete Nb_3Sn nucleation was observed and secondly the purity of the niobium substrate deteriorated significantly due to oxygen diffusion into the niobium during the high temperature treatment. We have therefore investigated the influence of various processing parameters on the Nb_3Sn coating and the thermal conductivity of the underlying niobium [14]. The most important modification applied to our standard diffusion process consisted in the introduction of a titanium shield around the cavity (Fig. 1).

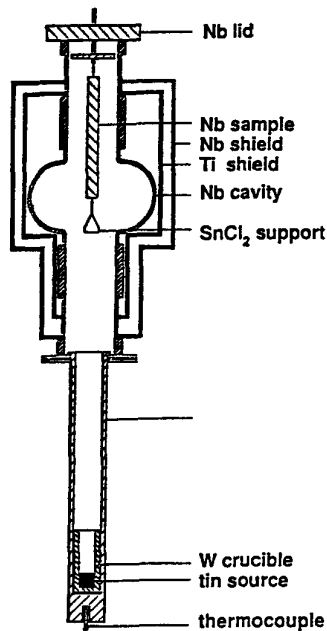


Fig. 1:

Nb_3Sn reaction chamber for the 3 GHz cavity. The surrounding separate heating systems for the tin source and the cavity as well as the UHV chamber are omitted for simplicity.

This shield acts as an oxygen getter during the high temperature treatment of the cavity. During the Nb_3Sn formation at 1100°C only a very thin Ti layer (less than 10 nm per hour) is formed which is not sufficient for the postpurification of the cavity. As the cavity inside is closed off by a niobium lid during high temperature processing no titanium can reach the rf surface of the cavity. Aside of this introduction of a getter shield the importance of other parameters, like the processing time and especially the tin vapor pressure, have been investigated. Finally a dense Nb_3Sn layer could be obtained on a high purity niobium substrate. After this optimization, the modified vapor diffusion technique has been applied to a spherically shaped 3 GHz cavity which was originally fabricated from reactor-grade niobium. Before this Nb_3Sn treatment the cavity was thoroughly investigated in regard to its performance as a niobium, and Nb_3Sn cavity of low RRR. It was at first chemically polished locally repaired and annealed in an UHV furnace at temperatures up to 1850°C several times. A maximum quench accelerating field of $E_a = 7.3 \text{ MV/m}$ and low field Q_0 values of up to $7 \cdot 10^{10}$ were achieved [15]. It was then coated with the standard vapor diffusion technique resulting in a quench limited accelerating field of 7.2 MV/m and a Q_0 of $5 \cdot 10^9$ at low fields [16]. After this series of experiments we have applied our modified vapor diffusion process. The cavity was first purified by the Titanium getter technique which improved its RRR value from 30 to 156. It was then covered with a $0.6 \mu\text{m}$ Nb_3Sn layer. The final surface treatment consisted of one oxypolishing at 65 V, an extensive rinsing with demineralized, dustfree water and an additional rinsing in dustfree methanol.

The cavity was then mounted onto a standard cryogenic rf test system under laminar airflow conditions. The resulting Q_0 versus E_a curve is shown in Fig. 2 in comparison to results of the earlier Nb₃Sn experiments with the same cavity (but with RRR = 30). The new coating technique resulted in an improvement of the accelerating from the 5 MV/m observed typically with low RRR cavities to almost 10 MV/m. Further experiments with thicker ($\approx 1 \mu\text{m}$) Nb₃Sn layers and repaired surface defects are planned for the future.

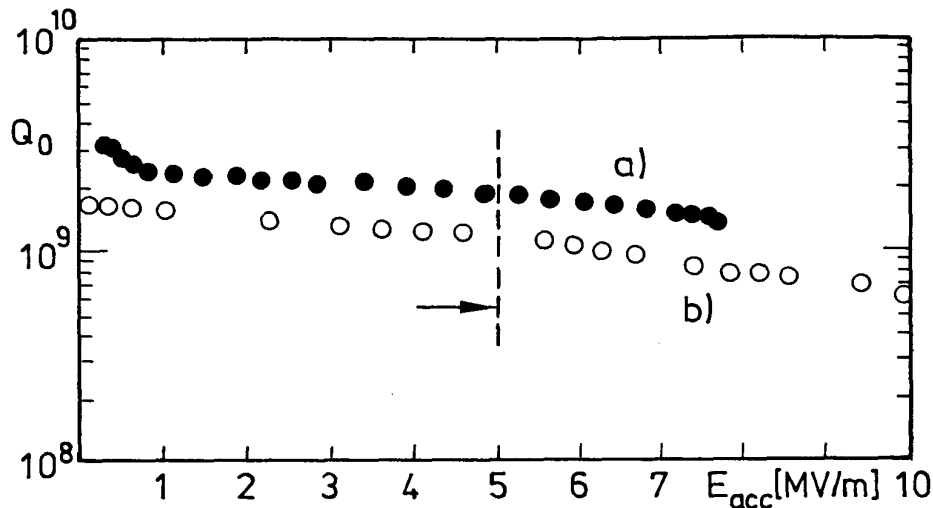


Fig. 2: $Q_0(E_a)$ dependence for the low (a) and high (b) purity Nb₃Sn cavity at 4.2K and 3 K. Shown is the best result for low purity material (curve a). More typical are maximum E_a fields around 5 MV/m (dashed line).

A few interesting questions regarding the physical properties of our Nb₃Sn layers remain to be answered. Do the 1 μm thick Nb₃Sn layers on niobium substrates have the same superconductivity parameters as bulk Nb₃Sn? What is their T_c and H_{c2} and how homogeneously have they formed? These questions can be answered by a magnetic shielding experiment [17]. The set up for such an experiment is shown schematically in Fig. 3. Two small coils (5 mm inner and 9 mm outer diameter and a length of 5 mm with 760 windings of 0.1 mm copper wire) face each other in a Helmholtz coil like arrangement with a distance from each other variable between 2 and 20 mm. Samples of typically 1 to 2.5 cm in diameter are placed between these coils. The source coil produces an a.c. magnetic field with an amplitude of typically 60 mOe at the location of the sample. If the sample is normal conducting the magnetic field penetrates it and induces a voltage in the pick up coil which is measured by means of a lock in amplifier. The arrange-

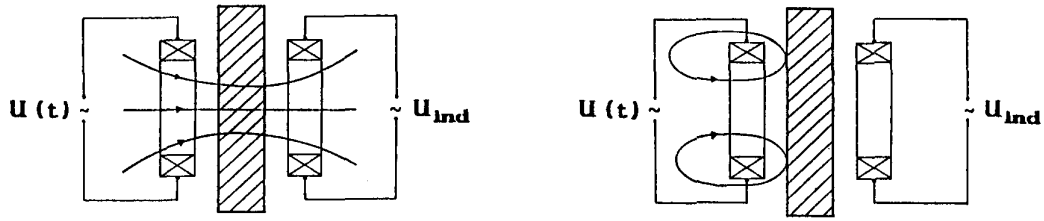


Fig. 3: Schematic set up of the magnetic shielding experiment to measure T_C and H_{C2} superconducting samples.

ment is placed in the field of a superconducting solenoid with a maximum excitation of 8 Tesla. The ambient temperature can be changed between 1.3 and 300 K. When the temperature falls below T_C the sample goes superconducting and acts as a magnetic mirror in respect to the source coil so that the induced voltage in the pick up coil drops strongly as seen in Fig. 4 for a high purity niobium sample.

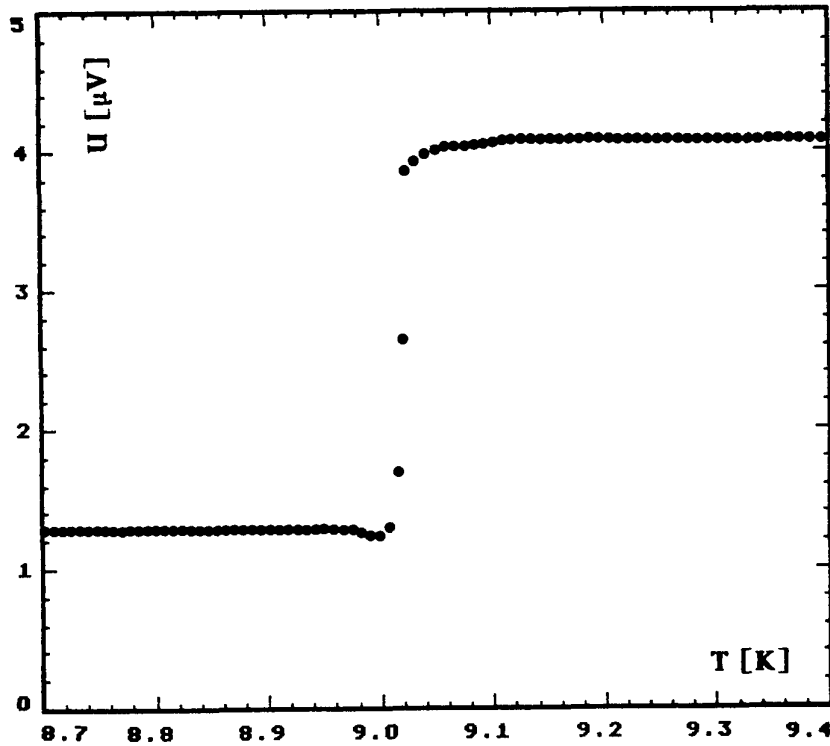


Fig. 4: Inductive T_C measurement on a high purity ($RRR = 110 \pm 30$) niobium sample.

The steepness of the transition is a measure for the homogeneity of the sample. The remaining signal below $T = 9.0$ K is due to the finite size and therefore incomplete magnetic shielding by the sample. Leaving the temperature at a constant level and increasing the applied magnetic dc field H results in a magnetic transition to the normal conducting state as shown in Fig. 5. Using this method the transition

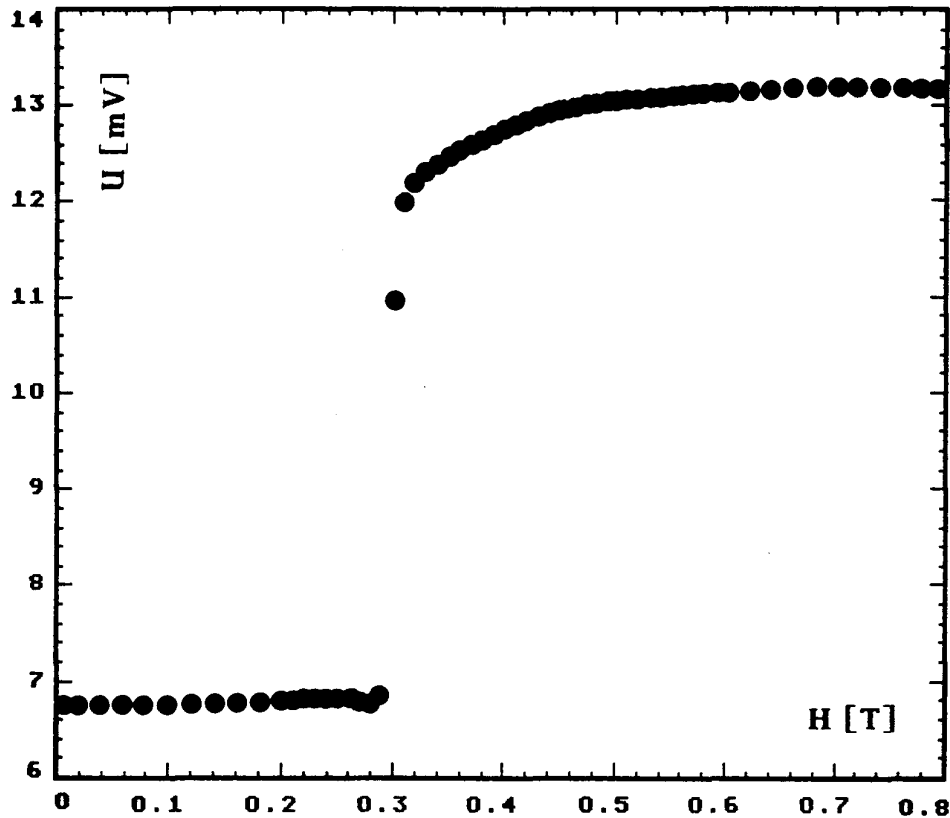


Fig. 5: H_{C2} -transition observed on a high purity niobium sample (RRR = 110) at 4.2 K.

field H_{C2} can be determined as a function of temperature. The measured $H_{C2}(T)$ curve is shown in Fig. 6. In the full temperature range the validity of the Abrikosov-Ginzburg-theory for superconductors in the pure limit ($\ell / \xi_0 \rightarrow \infty$) could be verified. The same measurements were carried out with a Nb_3Sn layer $0.6 \mu m$ on high

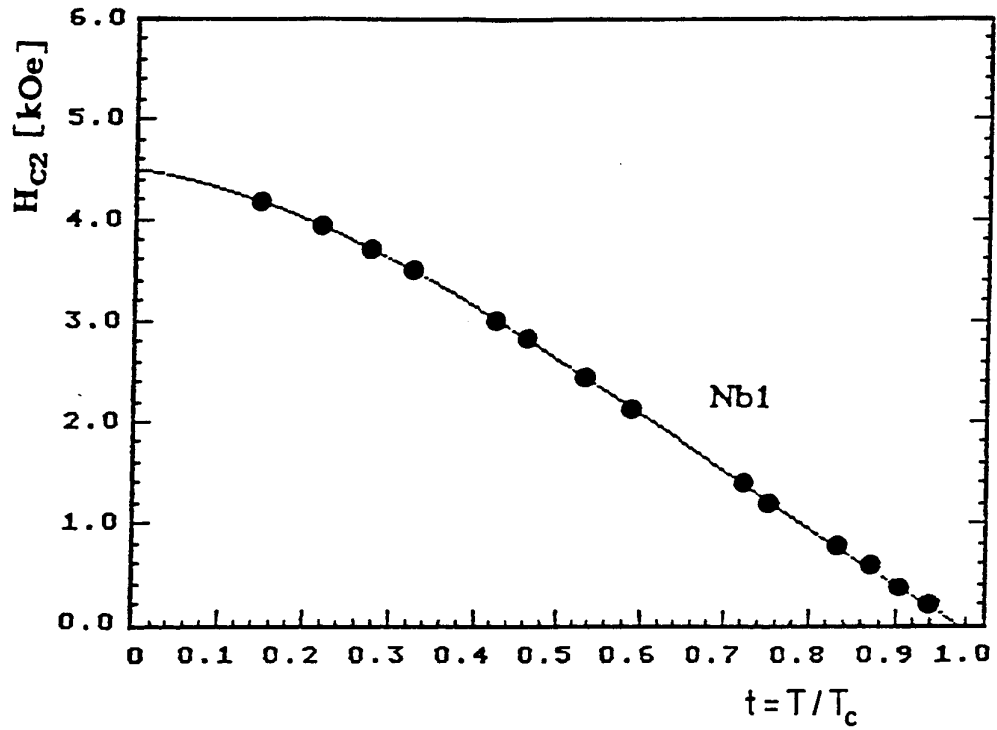


Fig. 6: Temperature dependence of H_{C2} of a high purity niobium sample.

purity niobium. The results are displayed in Fig. 7. T_C is measured at different values of the applied field. The sharp transitions indicate a good homogeneity of

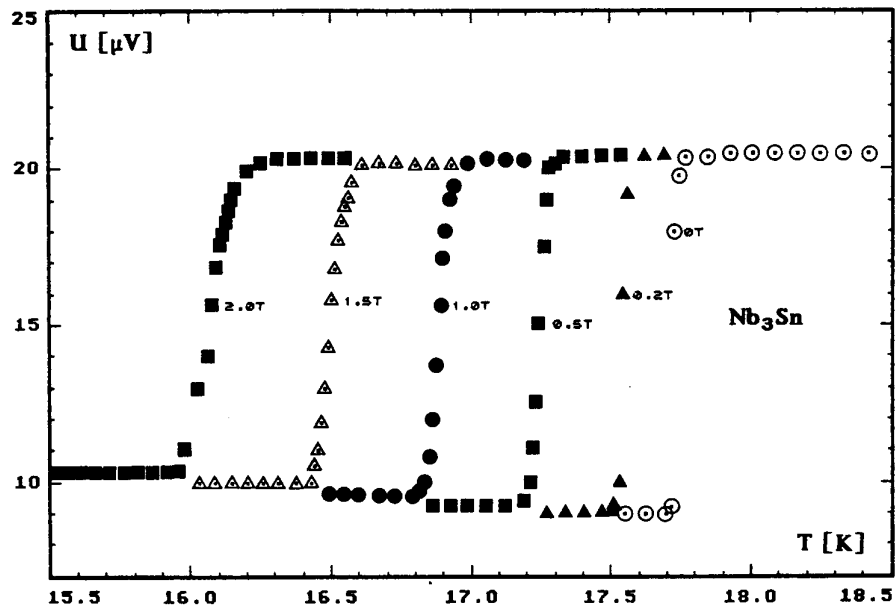


Fig. 7: Inductive T_C measurements in a varying external magnetic field on a Nb_3Sn layer on high purity niobium. ($0.6 \mu m$, $RRR = 144 \pm 7$)

even very thin Nb₃Sn layers produced by the vapor diffusion process. We have measured H_{c2}(T) for applied fields between 0 and 8 T and determined H_{c2}(0). Depending at what relative height of the pick up signal H_{c2}(T) is determined we obtain for two different Nb₃Sn layers of different thickness the results given in table 1.

Table 1

Nb ₃ Sn : (S1),1.5μm	Nb ₃ Sn: (S3),0.6μm
$\langle H_{c2}(0)_{90\%} \rangle = 20.44 \pm 0.15$ T	$\langle H_{c2}(0)_{90\%} \rangle = 21.15 \pm 0.14$ T
$\langle H_{c2}(0)_{50\%} \rangle = 20.34 \pm 0.15$ T	$\langle H_{c2}(0)_{50\%} \rangle = 20.42 \pm 0.13$ T
$\langle H_{c2}(0)_{10\%} \rangle = 19.89 \pm 0.14$ T	$\langle H_{c2}(0)_{10\%} \rangle = 19.68 \pm 0.12$ T

H_{c2}(0) results obtained on high purity Nb₃Sn scatter between 20 and 22 T and are in excellent agreement with our results on Nb₃Sn films.

3. Postpurified Niobium cavities at high fields

The threshold accelerating field in a superconducting linear collider to be competitive with proton storage rings like SSC and LHC at the high energy physics frontier is about 30 MV/m [18]. At such high fields Q₀ values around 10¹⁰ are required to reduce the refrigeration power and thereby increase the affordable luminosity. At present niobium cavities offer the most advanced technology to satisfy this challenge. Their ultimate performance will be given by the superheating magnetic field and the BCS surface resistance, which are at 1.7 K about 200 mT and 10nΩ at 3 GHz [19] the present design frequency of a superconducting linear collider [20]. For the usual π-mode accelerating structures these values correspond to accelerating fields of 45 MV/m and Q₀ values around 2.5 · 10¹⁰. Present days accelerating fields in large sized accelerating cavities [23] are between 5 and 10MV/m. Under optimized laboratory conditions accelerating fields approaching 25MV/m have been obtained repeatedly at 1.5 [21] and 3 GHz [22] in single cell cavities. During the past ten years major progress has been made in understanding the observed anomalous field limitations. In summarizing, microscopic particles of foreign material imbedded in the bulk niobium or loosely connected to its surface were found to be responsible for the observed electron field emission at relatively

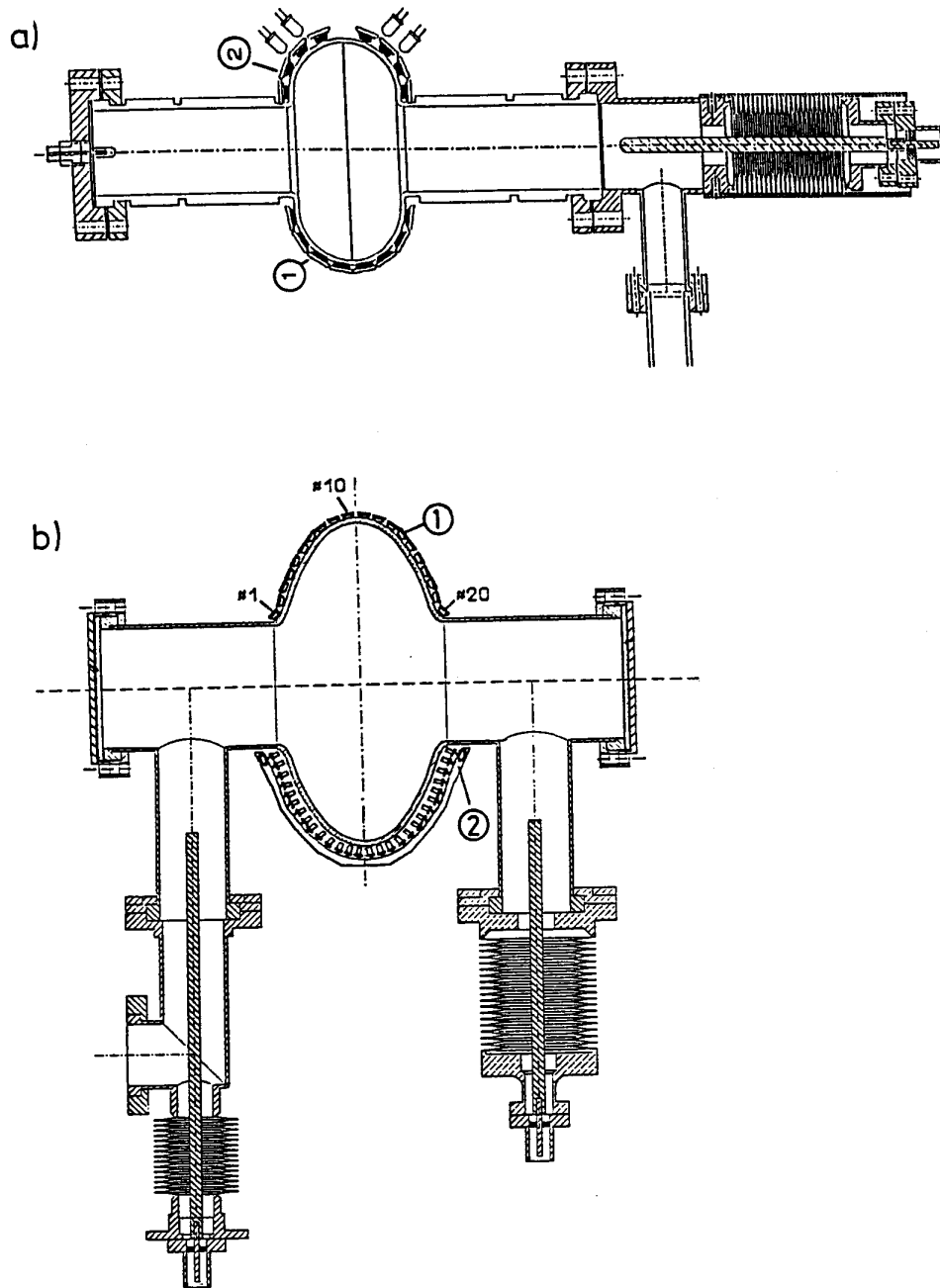


Fig. 8: Schematic drawing of the 3 GHz (a) and 1.5 GHz (b) cavities including variable rf couplers, Allen Bradley resistor thermometers (1) and photodiodes for x-ray detection (2).

low surfaces fields and for creating thermal instabilities by excessive local rf heating. D-C-field emission studies on niobium samples have shown that emission free surfaces (for electric fields up to 200 MV/m) can be obtained by high temperature firing at around 1400°C [24]. Guided by these observations we have in the last two years improved our clean room techniques, we have started to apply high temperature treatments to high purity niobium cavities close to 1400°C without seriously affecting their thermal conductivity and we have improved our diagnostic systems to investigate loss mechanism at fields above 10 MV/m in cavities immersed in superfluid helium. All our high field investigations were carried out with single cell 1.5 and 3 GHz cavities. They are shown in Figs. [8a] and [8b] together with their rf couplers and diagnostic tools. Because of the small size of our cavities all mounting steps after the removal of the last liquid fill are performed on a laminar flow work bench (working area 0.4 x 2 m²) of class 100, which is located in a dedicated clean (class 10000) and air conditioned room (2 x 3 m²). This small clean laboratory can be entered through a dressing room where clothing has to be changed. All our operations on the clean bench are monitored by a particle counter (typ HIAC/ROYCO Mod. 5120; $\geq 0.2 \mu\text{m}$). First and exploratory experiments to count the particles in the final cleaning liquids - dustfree water or methanol - have begun. Several unexpected dust contamination sources have been found and the mounting procedure was optimized. Thereby the onset surface field for detectable field emission loading could be increased to peak electric surface fields E_p beyond 41 MV/m (corresponding to $E_a = 16 \text{ MV/m}$) for our 3 GHz single cell resonators. The best results are $E_p = 63.8 \text{ MV/m}$ at $Q_o = 8 \cdot 10^9$ for a wet treated resonator and $E_p = 69.4 \text{ MV/m}$ at $Q_o = 4.5 \cdot 10^9$ for heat treatment as final preparation step. Finally we found good results to be much more reproducible than in earlier times.

Table 2 gives an overview over the five best results obtained with 3 GHz single cell cavities. The small scatter of these results around an average magnetic peak field of 100 mT may indicate that the remaining impurities on the cavities rf surface are intrinsic to the niobium material.

Table 2: Overview over the best results obtained with 3 GHz cavities of high purity

Number of cells	Cavity	Q_o (max) $\cdot 10^9$	Q_o ($0.95H_p$) $\cdot 10^9$	H_p [mT]	E_p E_{acc} [MV/m]		Limit	preparation before DFM
1	SW1B	8	1.5	96	59	23	FE	850°C
1	SW2	6	2.2	102	62.8	24.6	FE,Q	
1	S3A	30	10	105	63.8	25	Q	2*Ti,BCP50 H ₂ O,Meth
1	S3B	7	4.5	113	69.4	27.2	Q	1*Ti
5	E5	12	1.5	52	39	12.6	FE	2*Ti,BCP50
20	C20	5	1	28	20.8	6.7	FE	2*Ti,BCP50 H ₂ O
20	D20	3	1.7	33	24.3	7.8	Q	1*Ti

Table 3 shows the results of the best six experiments performed with 1.5 GHz single cell cavities. Shown are the data for the TM₀₁₀ and the TE₀₁₁-mode at 1.5 and 2.9 GHz respectively. In the TE₀₁₁ mode the average field is 80 mT and 44mT.

Table 3: Results of the six best experiments performed with 1.5 GHz single cell cavities

Test No.	f [MHz]	Q_o low field	Q_o high field	H_p [mT]	Quench # / angle
L 1-1	1490.62	$1.5 \cdot 10^{10}$	$6.1 \cdot 10^9$	42.7	10 / 80°
	2919.61	$1.7 \cdot 10^{10}$	$8.5 \cdot 10^9$	61.1	- / -
L 1-2	1490.53	$8.0 \cdot 10^9$	$4.4 \cdot 10^9$	30.6	13 / 0°
	2919.69	$2.3 \cdot 10^{10}$	$6.8 \cdot 10^9$	98.8	1 / 200°
L 1-3	1490.29	$1.1 \cdot 10^{10}$	$2.1 \cdot 10^9$	48.2	- / -
	2918.73	$2.4 \cdot 10^{10}$	$4.4 \cdot 10^9$	87.6	22 / 270°
L 2-1	1489.97	$1.3 \cdot 10^{10}$	$6.8 \cdot 10^9$	36.7	10 / 18°
	2917.87	$3.9 \cdot 10^{10}$	$2.7 \cdot 10^{10}$	93.8	1 / 170°
L 4-1	1473.57	$2.4 \cdot 10^{10}$	$2.6 \cdot 10^9$	47.2	- / -
	2853.23	$4.1 \cdot 10^{10}$	$3.5 \cdot 10^9$	68.1	not in cell
L 4-2	1473.57	$1.2 \cdot 10^{10}$	$2.5 \cdot 10^9$	60.9	14 / 195°
	2853.23	$1.3 \cdot 10^{10}$	$2.2 \cdot 10^9$	69.2	not in cell

in the TM_{010} -mode. The surface of this cavity is about four times larger than the one of a 3 GHz cavity which by a statistical argument may explain the observed reduction in the peak fields. It shall be pointed out, however, that none of the 1.5 GHz resonators has been heat treated or postpurified as yet. The systematic difference between the peak magnetic fields obtained in the TE and the TM-mode is as yet unexplained. It may indicate that a large number of the microscopic impurities on the cavity surface are dielectric in nature.

To obtain the high accelerating fields and quality factors listed in table 2 for our 3 GHz cavities the improved dust free mounting was important but not sufficient. High temperature annealing (HTA) was found to be essential. It homogenizes impurity clusters in the niobium material and thereby reduces the density of field emission sites, it removes oxides from the niobium surface and it leads to the evaporation of residues remaining on the cavity surface after chemical treatment. The large oxygen partial pressure in the hot zone of the furnace, however, leads to a diffusion of oxygen into the bulk niobium and therefore to a reduced thermal conductivity. The latter causes defect induced thermal instabilities at relatively low fields. Therefore, the solid state gettering process using a thin titanium layer evaporated on the inner and outer surface of the cavity was developed at Cornell to prevent the reduction or even foster the improvement of RRR during HTA. Due to the diffusion of the titanium into the niobium surface this treatment requires a final etching of at least 50 μm followed by an extensive water rinsing. There are strong hints that this additional wet treatment sacrifices again at least some of the positive effects of HTA. Moreover, the final etching produces a significant shift of the resonant frequency of the cavity. Especially in accelerator applications this may often be intolerable. Therefore, a new method was developed at Cornell [32] and Wuppertal [1] to post purify cavities by solid state gettering from the outside alone. Similar to the arrangement in Fig. 1 the cavity volume is closed off by niobium hats which block titanium atoms from reaching the inner part of the cavity on a direct path. The cavity is surrounded by a titanium sheet which in turn is well shielded against the furnace vacuum space by a niobium box. The resonator is heat treated at 1350°C for at least 18 hours. During this time a titanium layer forms on the outside of the cavity. It protects the resonator from oxygen emanating from the hot surfaces of the furnace. It also acts as a trap for the oxygen atoms within the cavity volume and the niobium bulk material. At 1350°C the oxygen is mobile enough within the bulk niobium to allow an effective diffusion into the titanium getter layer.

A 3 GHz cavity of medium purity which showed quenching at $E_a = 12$ MV/m was treated as described above. At first attempt an accelerating gradient of 27.2 MV/m ($E_p = 69.4$ MV/m, $H_p = 113$ mT) was achieved at a high field Q_0 of $4.5 \cdot 10^9$ without any detectable field emission loading. This cavity was removed from the UHV furnace under the protection of a laminar airflow. It was transported in a clean plastic container to our clean room and mounted without any further surface treatment. The "titanium box method" can be applied to complete accelerating structures and does not influence the resonant frequency of the cavity. The new process is therefore of great importance for the postpurification treatment of the S-band accelerating structures of the Superconducting Darmstadt Linear Accelerator. A first application to a 20 cell 3 GHz structure fabricated from RRR = 30 reactor grade niobium resulted in a very promising accelerating field of 7.8 MV/m [1]. The only draw back of this method is the observed reduction of the Q value of the treated cavities by a factor of about two. This disadvantage may be overcome by improving the process in the future.

Despite of this progress the understanding of the origin of anomalous losses in superconducting cavities at high fields remains to be a challenge as the theoretical field limits have not been reached. We have therefore continued the improvement of our diagnostic methods. The application of scanning thermometry in subcooled helium is limited to temperatures above the lambda point. At these temperatures the BCS surface resistance limits the thermal stability of cavities at high fields and though this diagnostic technique can only be used for peak magnetic surface fields $H_p < 67.5 \text{mT}/f[\text{GHz}]$. For 500 MHz this results in a comfortably high limit for H_p but at 1.5 and 3 GHz the present performance of the best single cell cavities asks for a thermometry in superfluid helium. Thermometers for this temperature range have been developed at Cornell [25] and we have adopted them for a scanning system where the thermometers glide over the outer surface of the cavity (Fig. 8 a and b). The measured temperature increase of this surface due to a heat source on the opposite rf surface of the cavity in the presence of the very effective cooling of the thermometer by the superfluid helium is only 5% of the real temperature increase. Figure 9 shows the spatial distribution of the temperature signal $\Delta T(x)$ measured with a thermometer sliding over a niobium

sheet (thickness: 2 mm) in superfluid helium at 1.4 K. The heat flux is produced by a heat input of 60 mW into an area of 5 mm in diameter on the opposite side of the niobium plate.

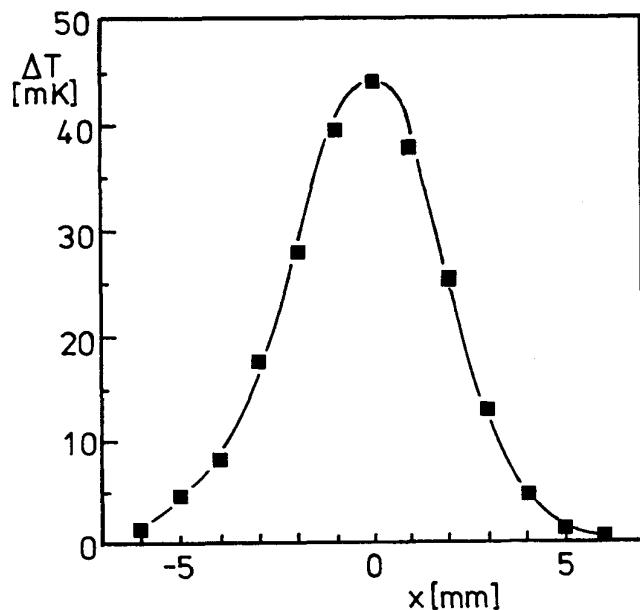


Fig. 9: Spatial distribution of the temperature increase $\Delta T(x)$ measured by a sliding thermometer on a niobium plate which is immersed in superfluid helium of 1.4 K. The heat flow is produced by an input of 60 mW into a 5 mm diameter spot on the opposite vacuum side of the niobium plate.

Identical thermometers were mounted on rotating frames (Figs. 8a,b) for a temperature cartography on 1.5 and 3 GHz cavities immersed in superfluid helium. These rotating frames were also equipped with a string of photodiodes sensitive to x-rays. The photodiodes work in principle like solid state ionisation chambers producing an output current proportional to the intensity of the Röntgen radiation produced by impacting electrons from field emitters on the cavity wall. Figs. 10 a and 10 b show a Röntgen and a temperature map of the 1.5 GHz cavity LI 4-2 at an accelerating field of 12 MV/m. Two field emitters are clearly visible. The intensity of the impacting field emitted electrons is very high in the cavity hemisphere where the emitter is located. There the strongly peaked radiation along the impact line occurs. The hemisphere opposite to the emitting site is bombarded strongly by secondary electrons which have a large angular spread and a much higher energy than the primary electrons. The large angular spread leads

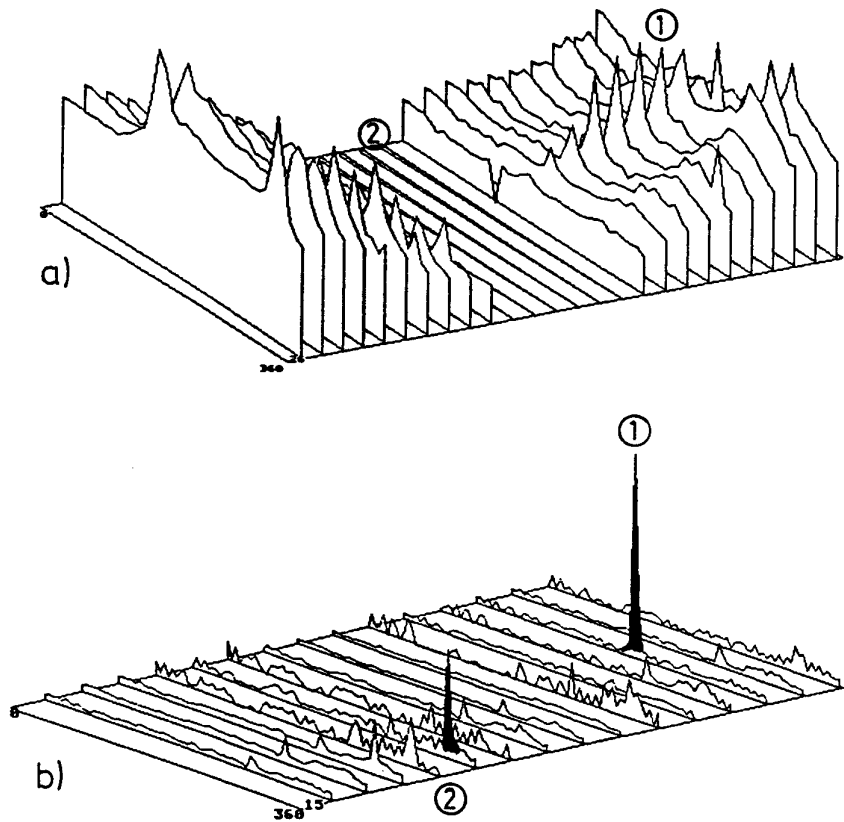


Fig. 10 : Electron emitters as seen in a Röntgen map (a) and in superfluid temperature cartography (b).

to a very broad maximum of Röntgen radiation opposite to the emitter site. Fig.11 shows a Röntgen map of the same cavity at a later time after five minutes of

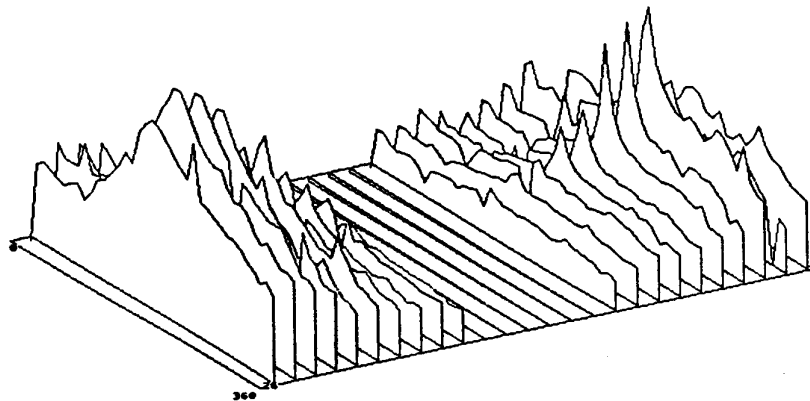


Fig. 11 : Röntgen map of cavity LI 4-2 at a later time compared to Fig. 10 and after 5 minutes of processing.

processing. There the peaked intensity of the primary electrons and the broad distribution of the x-rays from the secondary electrons is clearly seen as only one emitter remained after processing. The x-ray intensity at the broad secondary maximum is high because these x-rays are of high energy and penetrate the cavity wall easy. The temperature increase produced by the impacting electrons is not detected by the superfluid thermometry. At the location of the emitters, however, strong and very peaked temperature signals are observed. This indicates that the field emission observed in this case originates from hot emitters. This agrees with the frequently made observation that field emission from emitters on the cavity surface is accompanied by light emission characteristic for a glowing particle. Figures 10 and 11 show what kind of results one can obtain with scanning x-ray and temperature sensores in superfluid helium. Systematic studies are planned for the future.

4. A High T_C Cavity for a Compact Hydrogen Maser.

Since its first operation in 1960 [26] the hydrogen maser has proven to be useful both as a spectroscopic tool and as a frequency standard. To understand the principal of operation of such a maser the original work of Goldenberg, Kleppner and Ramsey is cited:

"A diagram of the apparatus is given in Fig. 12. Atomic hydrogen from a Wood's discharge source passes through a six-pole state selecting magnet which focuses atoms in the $F = 1, m = 0$ and $F = 1, m = 1$ states onto an aperture in a paraffin-coated quartz bulb. The bulb is located in the center of a cylindrical rf cavity, operating in the TE_{011} mode, which is tuned to the ($F = 1, m = 0 - F = 0, m = 0$) hyperfine transition frequency, approximately 1420.405 Mc/sec. The conditions are such that the atoms spontaneously radiate to the lower hyperfine level while in the bulb. The atoms make random collisions with the paraffin-covered bulb wall and eventually leave the bulb through the entrance aperture. Due to the small interaction with the paraffin surface they are not seriously perturbed for at least 10^4 collisions.

The criterion for self-sustained oscillation is that the power delivered to the cavity by the atomic beam must equal that lost by the cavity. In our case, with an average interaction time of 0.3 sec and a loaded cavity $Q = 60\ 000$, the minimum

beam flux needed for oscillation is $4 \cdot 10^{12}$ particles per second. The maximum power delivered to the cavity by this beam is approximately 10^{-12} watt."

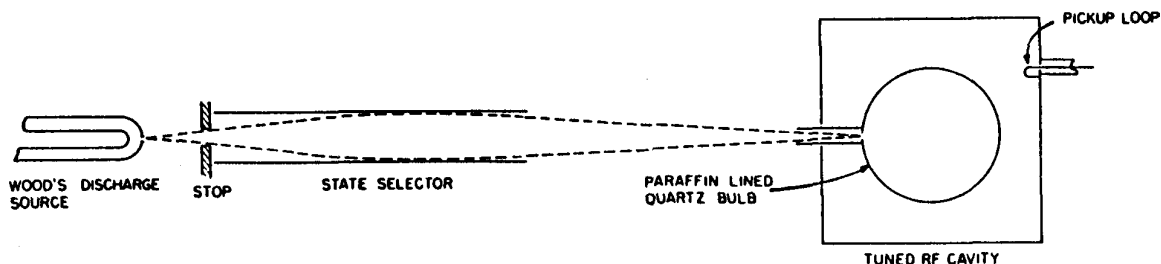


Fig. 12: Schematic diagram of atomic hydrogen maser.

The theory and the techniques of the hydrogen maser are described in references [27] and [28]. One of the most important applications of a hydrogen maser is its use as a stable clock. One of the interesting applications of highly stable clocks is their use in a global positioning system [29] which presently makes use of cesium beam atomic clocks. An exchange of these clocks against hydrogen masers could improve the precision of the system significantly. The development of a compact superconducting cavity hydrogen maser was therefore proposed by V. Folen and S. Wolf of the Naval Research Laboratory in Washington. They proposed to replace the very long TE_{011} cavity (diameter - height = 31 cm) by a compact cavity similar to that originally suggested by V. Folen for a conventional compact maser and to fabricate this cavity from high T_C superconducting material. On the basis of this proposal a collaboration between the Physics Department of the College of William and Mary, the Naval Research Laboratory and our group at Wuppertal is starting to develop such a cavity. It will be the central part of a compact hydrogen maser schematically shown in Fig. 13. The cavity will be made out of silver which is coated electrophoretically with $YBa_2Cu_3O_{7-\delta}$ following a procedure discussed in reference [11].

The size of the microwave cavity is given by a cylindrical copper shield which has an inner diameter of 7.5 cm and an equal inner height. The frequency and field distribution of the cavity are determined by the two electrodes which form a

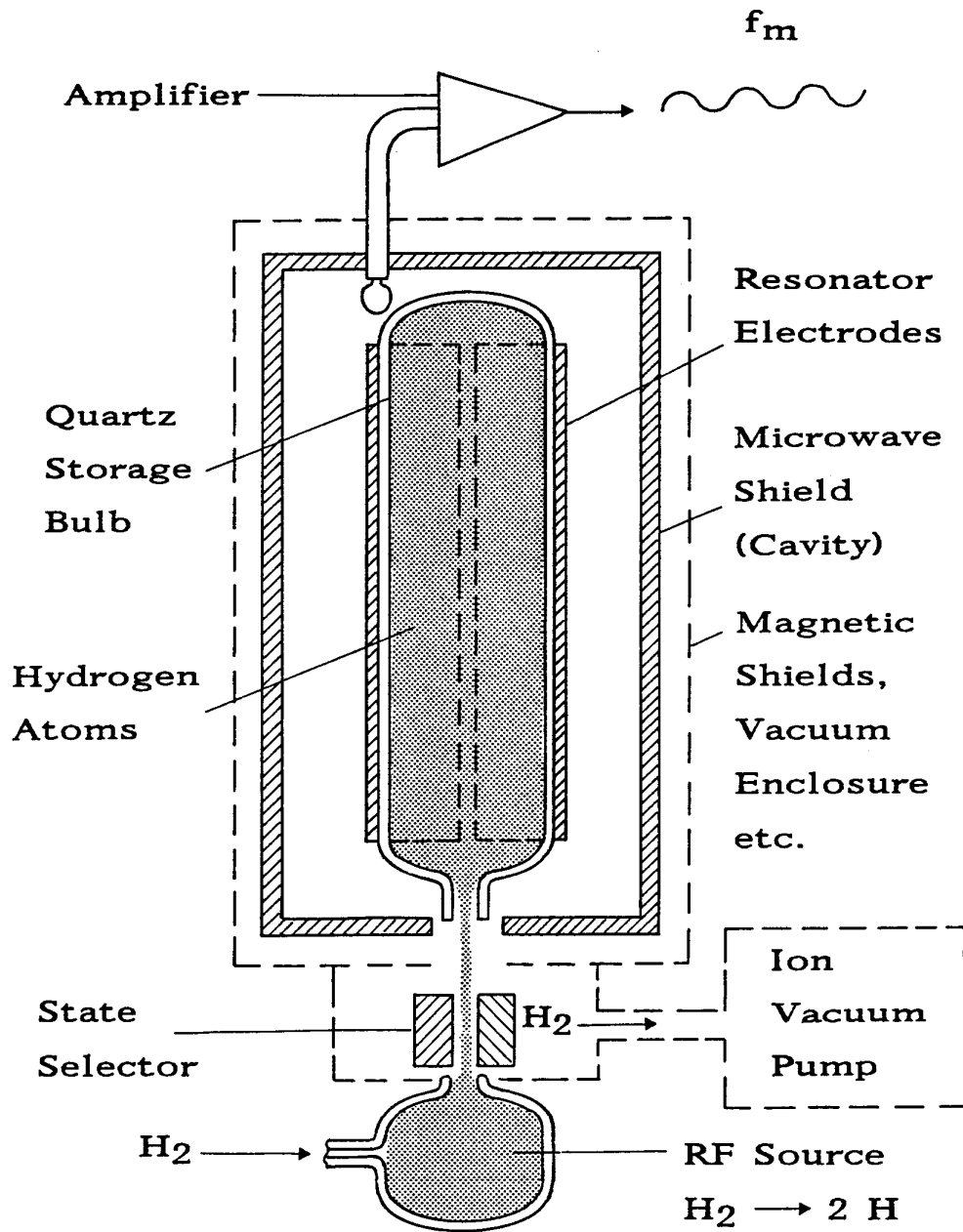


Fig. 13 : Schematic of a compact hydrogen maser (from reference [29]).

resonant circuit as shown in Fig. 14. These have the form of two adjacent half cylinders (5 cm in diameter and 5 cm high with a gap of 0.4 cm) and cover the quartz storage bulb.

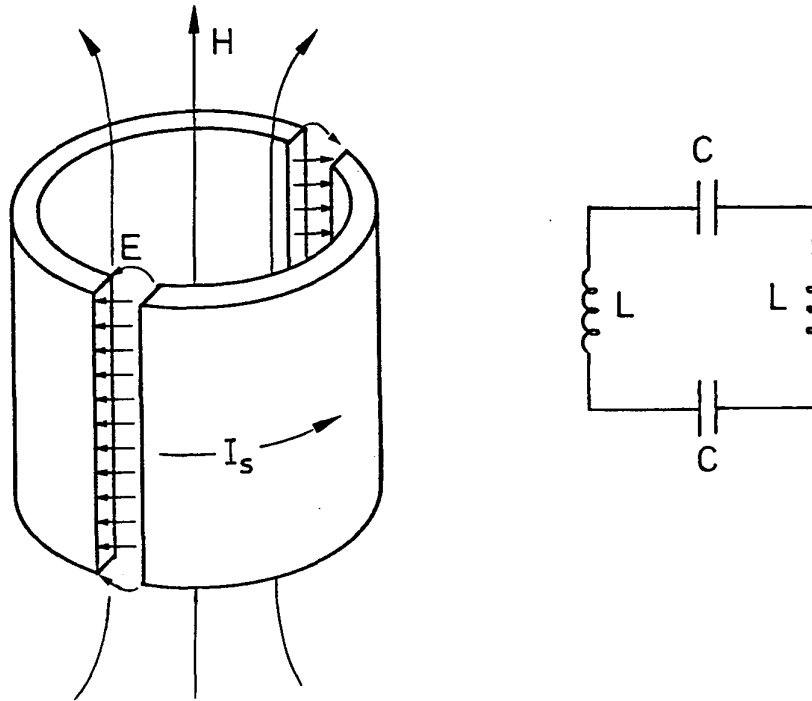


Fig. 14 : The resonant electrode system of the compact microwave cavity and its equivalent circuit.

The cylindrical copper shield around the two electrodes merely prevents energy loss by radiation. About 80% of the microwave losses occur on the inner electrodes. The cavity Q is given by:

$$Q^{-1} = \frac{R_s^E}{G_E} + \frac{R_s^S}{G_S} \quad (5)$$

where G_E and R_s^E are geometry constant and surface resistance of the electrodes and G_S and R_s^S are the equivalent quantities for the shield. The first prototype of a superconducting cavity is shown in Fig. 15. For this cavity G_E and G_S are 60 and 200 Ω respectively.

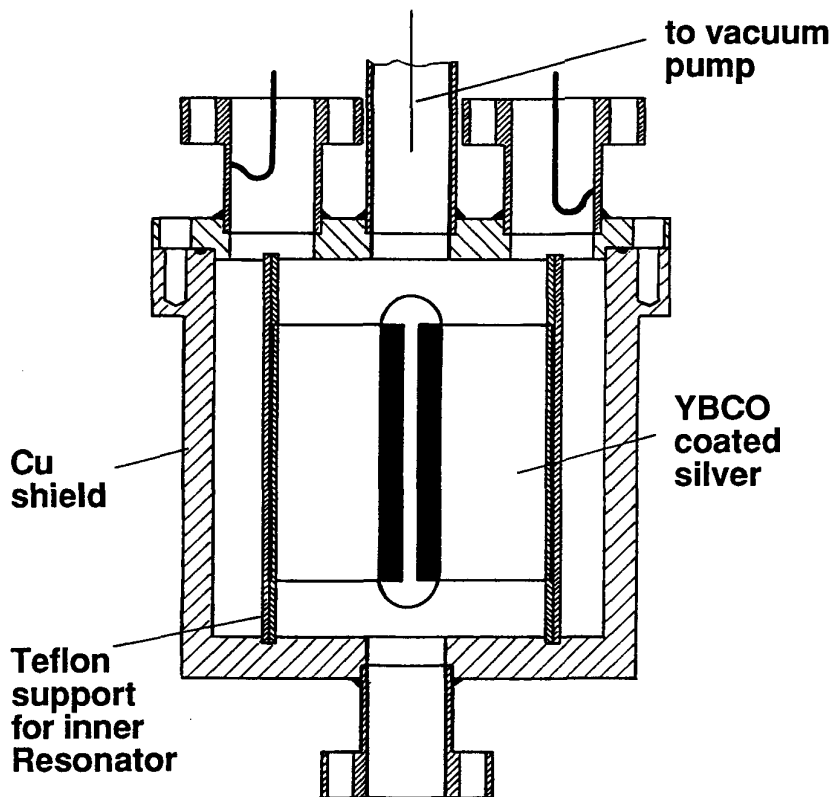


Fig. 15: Prototyp of a superconducting compact maser cavity.

In a first experiment we have replaced the normal conducting electrodes which contribute most to the microwave losses by silver electrodes electrophoretically covered by a $\text{YBa}_2\text{Cu}_3\text{O}_{7-\delta}$ layer of 20-30 μm thickness. The copper shield will be of silver coated with YBCO in a later experiment. The cavity of Fig. 15 was mounted to an appropriate cryogenic test system within a cryostat.

The interior of the cavity was evacuated and then filled with low pressure helium gas (10^{-3} mbar at 4.2 K) to provide a thermal contact between the inner electrodes and the copper shield. The cavity was cooled to 4.2 K by filling the cryostat with liquid helium. Then the helium was removed and the cavity warmed up very slowly to room temperature within 48 hours. The temperature of the

cavity was monitored by a platinum resistor thermometer and the cavity Q was determined by a computer controlled sweep off the drive frequency and by measuring the full width at half maximum of the resonance curve of the field amplitude in the cavity. The results of the first two experiments are given in Fig. 16. The

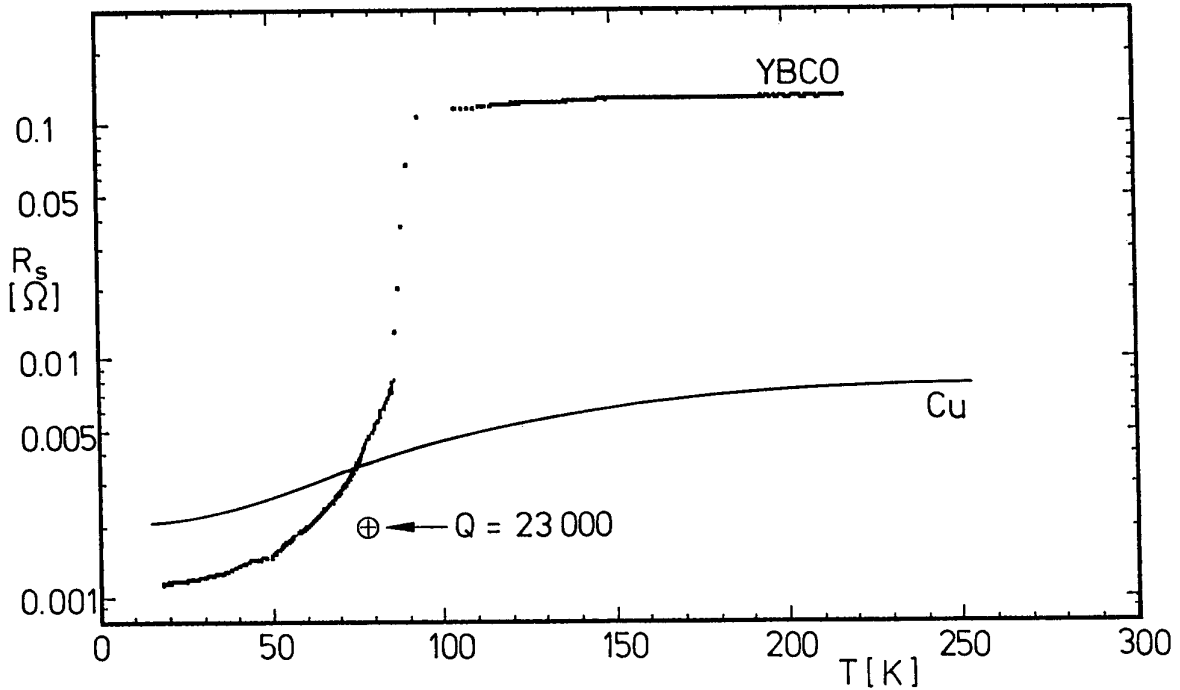


Fig. 16 : Temperature dependence of the surface resistance of the inner electrodes of the maser cavity as a function of temperature compared to the temperature dependence of R_s of copper measured in the same cavity where the YBCO electrodes were replaced by copper electrodes. The curve of YBCO data points are from our first experiment. The single data point was the result of a second YBCO coating of the electrodes.

surface resistance of the YBCO covered inner electrode is derived from equation (5). The temperature dependence of the surface resistance of copper was determined in the same cavity after replacing the YBCO covered electrodes by copper ones.

The temperature dependence of the surface resistance of the YBCO electrodes shown in Fig. 16 was measured after the first coating and after frequent handling of the electrodes. After a second YBCO coating a surface resistance of 2 mΩ at 78 K was reached which corresponds to a Q of the maser cavity of 23000. This is to be compared to a Q of an equivalent copper cavity at room temperature of 5000. For the maser operation a Q value at 78 K of 40 000 has to be achieved. With further improvements of our coating technique this value should be obtainable. On 2.5 cm diameter samples at 21.5 GHz 80 mΩ were obtained at 78 K (with an untextured surface). Scaling this result with a quadratic frequency dependence to 1.42 GHz gives a surface resistance of .35 mΩ or an equivalent Q of the maser cavity of $9.45 \cdot 10^4$.

5. A Superconducting Pendulum Gravimeter

The ongoing discussion about the existence of a short range modification to Newtons law of gravitation has influenced us to start the development of a pendulum gravimeter which is planned to use a superconducting Fabry-Perot cavity as its main element. Such a gravimeter would be a new method different from the one used in the classical Cavendish experiments to determine the absolute value of the gravitational constant [31].

A Fabry-Perot resonator generally consists of two oppositely faced metallic mirrors as shown for example in Fig. 17. As first described in the work of Boyd and Kogelnik [30] the lowest diffraction losses occur for spherically curved mirrors near the confocal configuration where the radius of curvature R is equal to the mirror distance b.

This configuration however is not stable and one has to chose $b < R$. One finds that for a resonator with a minor diameter of $d = 13$ cm and $R = 46$ cm , b values of up to 15 cm result in diffraction losses at K-band frequencies which are negligible in comparison to the reflection losses at the superconducting mirror surfaces.

The frequency of the TEM_{mnp} -modes excited in a Fabry-Perot resonator is given to a good approximation by:

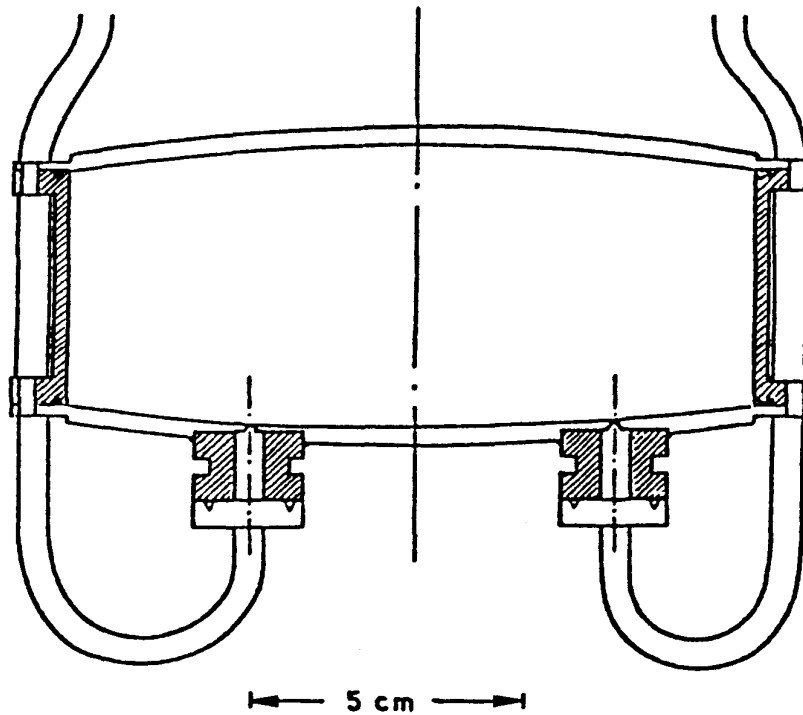


Fig. 17 : A Superconducting Fabry-Perot resonator.

$$f_{pmq} = \frac{c}{2b} \left(q + 1 + \frac{1}{\pi} \cdot (1+2p+m) \cdot \arccos(1-b/R) \right) \quad (6)$$

From this relation one can see that a superconducting Fabry-Perot resonator is an appropriate device for measuring small displacements Δb of the two mirrors in respect to each other, provided a Q characteristic for a superconducting resonator can be achieved. We have therefore designed and tested a superconducting Fabry-Perot resonator as a first step towards a pendulum gravimeter [31]. A Q value of $1.8 \cdot 10^7$ was obtained with the resonator shown in Fig. 17 where the two mirrors are fabricated from niobium and held apart by a copper cylinder. This Q value is more than a 100 times higher than the Q value of a corresponding copper resonator. After having obtained this result, we designed and constructed the normal conducting prototype of a pendulum gravimeter (Fig. 18).

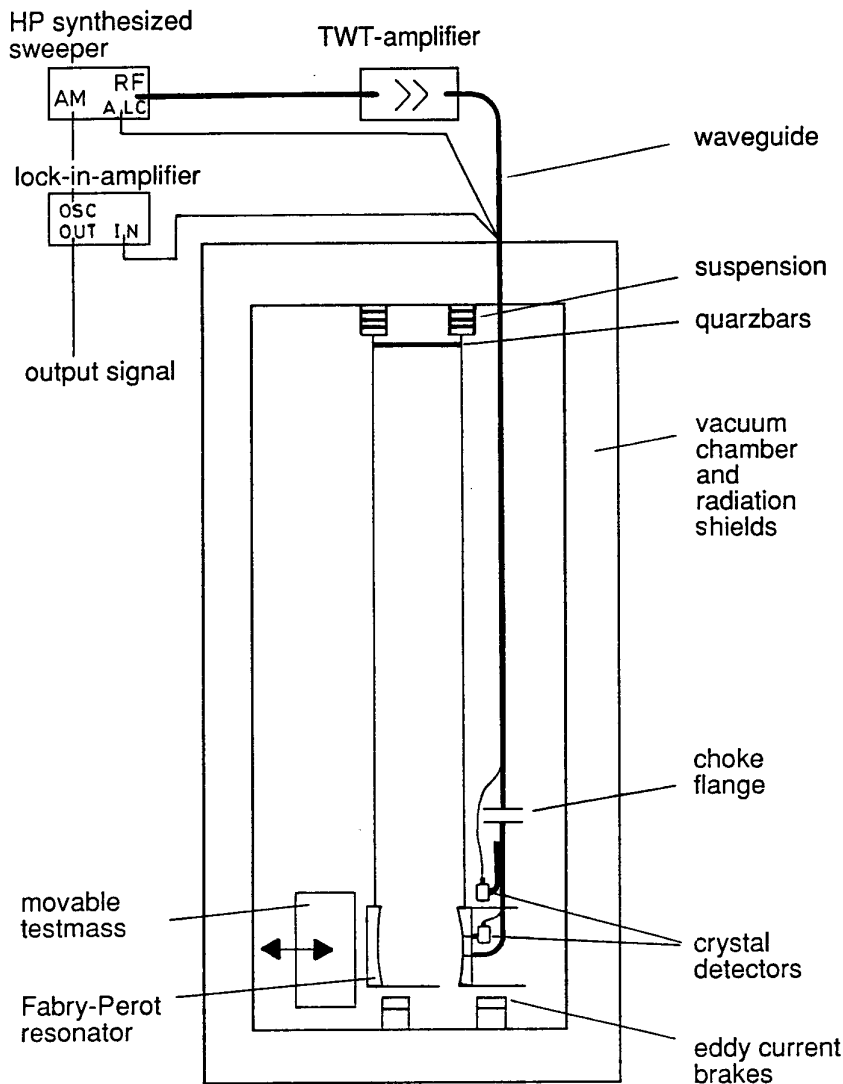


Fig. 18 : Experimental setup for the pendulum gravimeter based on a normal conducting Fabry-Perot resonator.

Two copper Fabry-Perot mirrors were suspended on tungsten wires in a vacuum chamber close to a test mass. The damping of the pendulum oscillations excited by microseismic forces was provided by eddy current brakes and by mounting the suspension platform on alternating layers of steel and rubber.

In order to reduce thermal expansion effects on the mirror distance sufficient thermal isolation of the mirrors by radiation shields was provided. In addition the spacing between the suspension points of both pendulums is fixed by bars of quartzglass. The microwaves were fed into the resonator by a waveguide which is mechanically separated from the mirror by a choke flange.

As a reference oscillator a HP Synthesized sweeper providing a frequency stability of a few Hz at 24 GHz was used. The amplitude was modulated with 1kHz. Setting the oscillator frequency to the 3 db point of a TEM resonance curve transforms small frequency changes into amplitude changes. The amplitude was measured with a crystal detector and a lock-in amplifier. In order to minimize drifting effects an ALC circuit was driven by a crystal detector in the input line in front at the choke flange. The dc voltage from the crystal detectors was transmitted by copper wires of 0.1 mm thickness to prevent vibrations. With this technique the resonance frequency can be measured with a relative precision of 10^{-10} .

Fig. 19 shows the transmitted signal versus time after passing a low-pass filter with a time constant of 12.5 s.

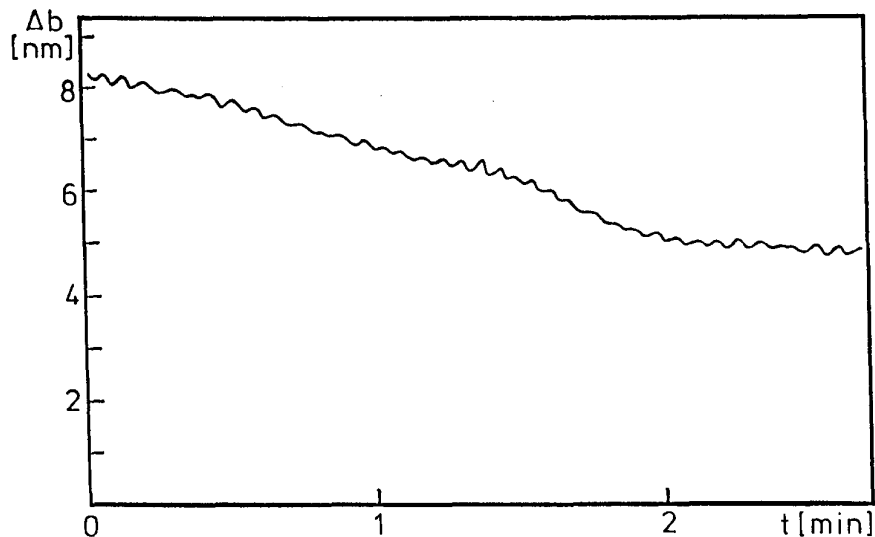


Fig. 19: Change of mirror distance versus time measured with the pendulum gravimeter.

The observed drift of 0.1 nm to 1 nm per minute could be reduced meanwhile to a value of 0.02 nm per minute over several hours by an improved thermal isolation. The residual microseismic amplitude is observed to be about 0.1 nm. An improved method to measure small frequency changes is a computer controlled scan of the resonance curve. So it is possible to eliminate the sensitivity against

the drift of the microwave amplitude and to suppress microseismic noise by applying a numerical filtering method. The digital frequency versus time data also allows the application of a Fourier analysis.

Fig. 20 shows the resonant frequency f_0 as a function of time over a space of 12 hours. The observed behaviour can be explained well by tidal forces which may be seen by comparing the computed curve (labelled primary tide).

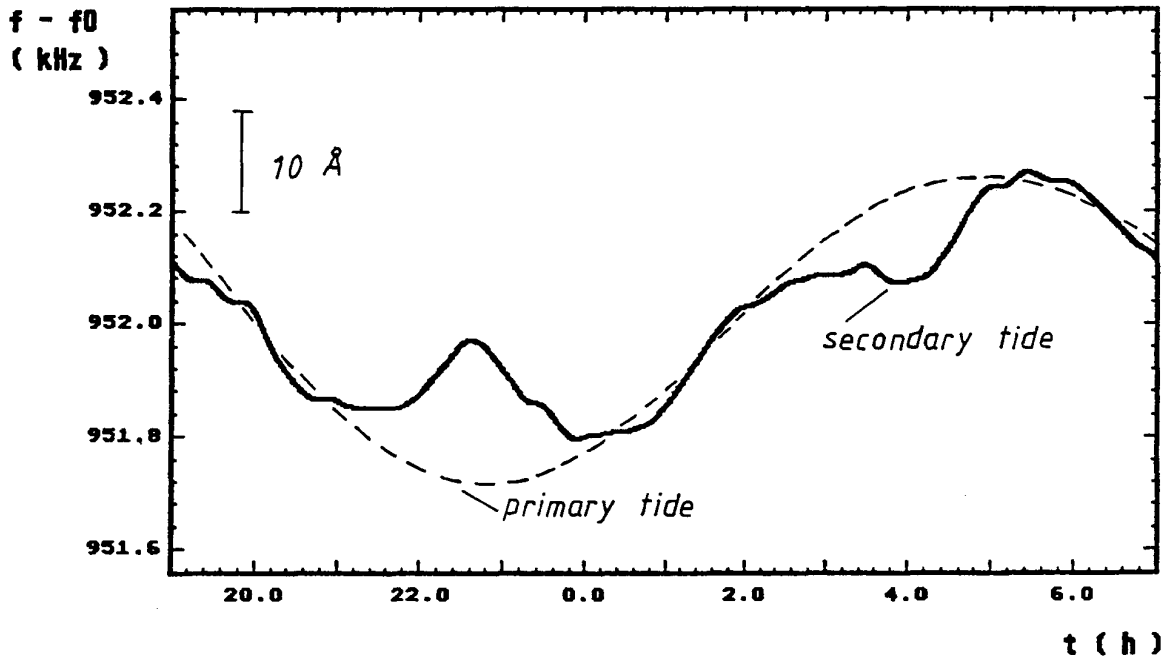


Fig. 20: Tidal forces observed on the 4th to the 5th of July 1987 with pendulum gravimeter prototype.

The deviation of a 3 m long pendulum out of its rest position by tidal forces is approximately 3000 \AA . As both pendula respond approximately equal this large effect is reduced to a relative deviation of two pendula against each other by 15 \AA which is seen in Fig. 20. The deviations from a sinusoidal curve which is observed is most likely due to the secondary tide which is produced by the change of the mass distribution of the earth, the oceans and the atmosphere due to the primary tides. Our experiments with the pendulum gravimeter have only just begun and will continue in the direction of the application of a superconducting Fabry-Perot. At present it is not decided if this will be a YBCO, Nb_3Sn or niobium resonator.

References

- [1] R.W. Röth, H. Heinrichs, G. Müller, H. Piel, J. Pouryamout, "Results of Post-purified Accelerator Structures", Proc. of the 4th Workshop on RF Superconductivity, KEK, Japan (1989).
- [2] H.Chaloupka, H. Heinrichs, A.Michalke, H. Piel, C.K. Sinclair, F. Ebeling, T. Weiland, U. Klein, P. Vogel, "A proposed Superconducting Photoemission Source of High Brightness", *ibid.* ref. 1.
- [3] G. Müller, "Microwave Properties of High- T_c Oxide Superconductors", *ibid.* ref. 1.
- [4] K. Alrutz-Ziemssen et al., "Performance of the Accelerator Cavities at the Superconducting Darmstadt Linear Accelerator (S-DALINAC)", *ibid.* ref. 1.
- [5] G. Rempe, H. Walther, N. Klein, "Observation of Quantum Collapse and Revival in a One-Atom Maser", *Phys. Rev. Lett.* 58, 353, 1987.
- [6] U. Klein and D. Proch, "Design Consideration for a 130 MeV Superconducting Recyclotron for Electrons", Proc. of the Conf. on Future Possibilities of Electron Accelerators, Charlottesville, 1979, J.S. McCarthy and R.R. Whitney, editors (Univ. of Virginia, Charlottesville), p. N1-17.
- [7] H.Piel, "Diagnostic Methods of Superconducting Cavities and Identification of Phenomena", Proc. of the Workshop on RF Superconductivity, Kernforschungszentrum Karlsruhe, 1980, M. Kuntze, editor, KFK 3019(1980), p.85.
- [8] G.Arnolds, H. Heinrichs, R. Mayer, N. Minatti, H. Piel, W. Weingarten, "Design and Status of an Experimental Superconducting Linear Accelerator for Electrons", *IEEE Trans.* NS-26, (1979), p.3775.
- [9] G. Müller, Dissertation University of Wuppertal, WUB-DI 83-1 (1983).
- [10] H. Padamsee, Proc. of the Second Workshop on RF Superconductivity, CERN, Geneva, Switzerland (1984), H. Lengeler, editor, p.339.
- [11] M. Hein, E. Mahner, G. Müller, H. Piel, L. Ponto, M. Becks, U. Klein, M. Peiniger, "Electrophoretic Deposition of Highly Textured $YBa_2Cu_3O_{7-\delta}$ Thick Films", *ibid.* ref. 1 and Proc. of the International M^2S -HTSC Conf. Stanford, Ca., July 23-28,1989, to be published in *Physica C*.
- [12] N. Klein, G. Müller, S. Orbach, H. Chaloupka, B. Roas, L. Schultz, U. Klein, M. Peiniger, "Millimeter Wave Surface Resistance and London Penetration Depth of Epitaxially Grown $YBa_2Cu_3O_{7-\delta}$ Thin Films", *ibid.* ref. 11.

- [13] M. Peiniger, M. Hein, N. Klein, G. Müller, H. Piel and P. Thüns, " Work on Nb₃Sn Cavities at Wuppertal, Proc. of the Third Workshop on RF Superconductivity, K. Shepard, editor, Argonne Nat.Lab. ANL-PHY-88-1 (1988).
- [14] D. Dasbach, G. Müller, M. Peiniger, H. Piel and R.W. Röth, "Nb₃Sn Coating of High Purity Nb Cavities", IEEE Trans. Magn. MAG-25, 1362 (1989).
- [15] H. Lengeler, W. Weingarten, G. Müller and H. Piel, IEEE Trans. on Magn. MAG-21, 1014 (1985).
- [16] M. Peiniger and H. Piel, " A Superconducting Nb₃Sn Coated Multicell Accelerating Cavity, IEEE Trans. on Nucl. Sci, NS-32, 3610 (1985).
- [17] E. Mahner, Diplomarbeit, University of Wuppertal, 1989, WU D-89-13.
- [18] M. Tigner and H. Padamsee, Proc. of the Third Workshop on RF Superconductivity, ed. by K. Shepard, Argonne Nat. Lab. ANL-PHY-88-1,1(1988).
- [19] G. Müller, *ibid* ref. [18]. p.331.
- [20] D.L. Rubin, J. Graber, W. Hartung, J. Kirchgessner, D. Moffat, H. Padamsee, J. Sears and Q.S. Shu, contribution to this workshop and CLNS 89/909, Cornell University.
- [21] Q.S. Shu, K. Gendrean, W. Hartung, J. Kirchgessner, D. Moffat, R. Noer, H. Padamsee, D. Rubin and J. Sears, Proc. of the Particle Accelerator Conf., Chicago, March 1989 (in press).
- [22] G.Müller, H. Piel, J. Pouryamout and R.W. Röth, "High Electromagnetic Fields at Low RF Losses in a Superconducting S-Band Accelerator Cavity", Proc. of the European Particle Accelerator Conference, Rome (1988),1289, editor, F. Tazzari.
- [23] Y. Kojima et al., "Laboratory Report on the KEK Activities", *ibid.*, ref. 1.
- [24] Ph. Niedermann, *ibid* ref. [18] , p.249.
- [25] P. Kneisel, G. Müller and C. Reece, IEEE Trans. on Magn. MAG-23, 1417 (1987).
- [26] H.M. Goldenberg, D. Kleppner and N.F. Ramsey, Phys. Rev. Lett. 5, 361(1960).
- [27] D. Kleppner, H.M. Goldenberg and N.F. Ramsey, Phys.Rev. 126, 603 (1962).
- [28] D. Kleppner, H.C. Berg, S.B. Crampton and N.F. Ramsey, Phys.Rev., 138, A972 (1965).
- [29] S. Wolf, Naval Research Laboratory, Washington D.C., private communication.
- [30] G.D. Boyd, H. Kogelnik, Generalized Confocal Resonator Theory, Bell. Syst. Tech. J. 41, 1342 (1962).
- [31] N.Klein, G. Müller, H. Piel, J. Schurr, "Superconducting Microwave Resonators for Physics Experiments", *ibid* ref. 14.
- [32] J. Kirchgessner et al., "Laboratory Report on the Cornell Activities", *ibid.* ref.1.